IRAQI Academic Scientific Journals

SAMARRA JOURNAL OF ENGINEERING SCIENCE AND RESEARCH

S.J.E.S.R

Resource allocation in a MIMO network with smart reflective surfaces by using deep learning algorithms

Suham A. Albderi[1*],

1- Al-Furat Al-Awsat Technical University, 31003, Najaf, Iraq

Article Information

Received: 21/07/2024

Accepted: 29/09/2024

Keywords:

Resource Allocation, Deep Learning, MIMO Networks, Intelligent Reflective Surfaces (IRS), Wireless Communication Systems, Dynamic Environment.

Corresponding Author

E-mail:
Kin.shm@atu.edu.iq
Mobile:
+9647819473163

Abstract

Recently, wireless communications systems have developed significantly, and have impacted the spread of intelligent reflective surfaces (IRS) in multiple-input-multi-output (MIMO) networks. However, efficient allocation of resources such as power, bandwidth, and number of antennas among users in these networks remains a major challenge. A deep learning-relied (DL) algorithm for resource allocation in MIMO networks with IRS is suggested in this study. The proposed algorithm exploits the power of DL to optimize resource allocation in real-time, taking into account channel conditions as well as client motion. The performance of the suggested algorithm will be evaluated by performing multiple large-scale simulations and comparing it to existing resource allocation algorithms in MIMO/IRS system. The results show that the proposed LSTM-RNN/DL algorithm outperforms similar algorithms in terms of spectral efficiency, accuracy, and convergence speed. This research contributes to the development of resource allocation techniques in MIMO networks with IRS for outstanding efficiency using MATLAB program. Simulation results show BER of 104 with 99.8% performance efficiency to cover the increasing demand for wireless communication services.

Introduction:

To expand productivity and wellbeing in underground mines, empower travellers and drivers in street and metro burrows, and forestall terrorist attacks by observing those susceptible locals, solid and proficient transmission lines are desperately required. Normal wave propagation-based remote networking is more adaptable and powerful than wire-based frameworks since it is reasonable, easy to utilize, and extensible. In any case, burrows are not great for the propagation of radio waves. At present, the GO model, the Waveguide model, and the Full Wave model are the three primary procedures used to address the channel properties of regular waves in burrows. The EM field in the cylinder is created in the GO model by adding the commitments of beams that experience reflections on the remember for and diffractions near burrow wedges. It is prepared to do numerically anticipating the sign postponement and course misfortune at any area. However, to characterize the climate, the GO model necessities a great deal of information. Furthermore, the incredibly big number of beams causes analytical issues for extended burrow courses, and the convergence might consume most of the day. A passage is seen as an expanded waveguide with deficiently lossy walls in the waveguide model. The waveguide model suggests there is only the lower mode signal propagation in the cylinder since the sign of higher request mode weakens extensively quicker than in the lowercase letters. Channel models are a fundamental part of correspondence frameworks, providing a numerical system to comprehend how data is sent over a correspondence channel [1-3]. A correspondence station can be any medium through which data is communicated, including wires, optical fibers, radio waves, and satellite connections. A channel model catches the way of behaving of the channel and gives a method for dissecting the presentation of a correspondence framework under various circumstances, like noise, impedance, and bending. The most widely recognized kind of divert model utilized in correspondence frameworks is the additive white Gaussian noise (AWGN) model. This model expects that noise added to the sign is Gaussian dispersed with zero mean and a consistent power otherworldly thickness. The AWGN model is broadly utilized on the grounds that it gives a basic and exact portrayal of some true channels, including remote channels, optical fibers, and a few sorts of wired correspondence channels. Different kinds of channel models incorporate blurring channels, multipath channels, and impedance channels, every one of which catches various parts of the channel conduct and can be utilized to examine various sorts of correspondence frameworks. A communications system is considered where the transmitter is located To communicate with the receiver, where this connection is with the assistance of a Large Intelligent Surface (LIS), as shown in Figure 1. These transceivers can represent either base User stations or equipment. The LIS is equipped with M Reconfigurable elements and assume that both the transmitter the receivers have one antenna. It is worth mentioning here such an assumption is made only for the sake of simplicity Presentation, suggested solutions and outcomes in this regard the idea might be simply extended to multi-antenna transceivers [8].

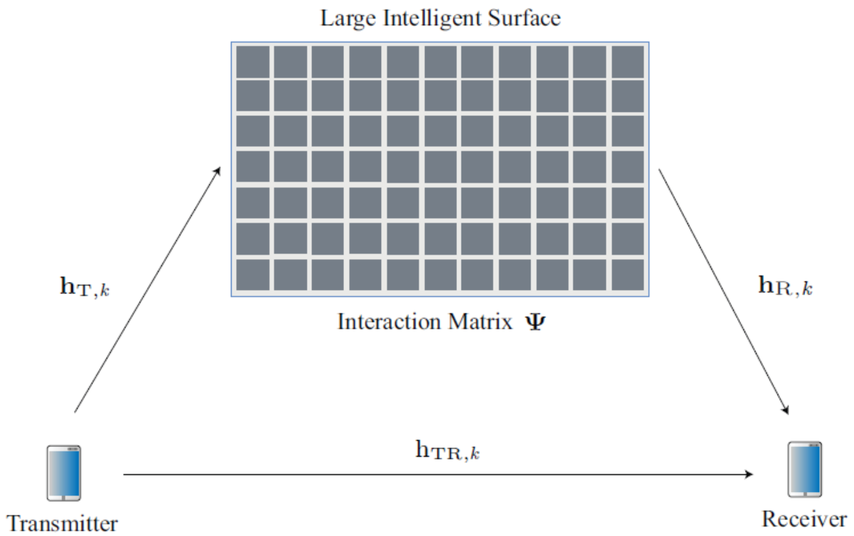

Fig. 1: *A diagram of the adopted system model whereas communication between sender and detector is supported by a large smart surface (no). The LIS reacts to the incident wave through matrix interaction [4].*

In this project, an OFDM based system is proposed with K subcarriers. We define hTR;k as the direct channel between the transmitter and receiver at the kth subcarrier, hT;k, hR;k as the M×1 uplink channels from the transmitter and receiver to the LIS at the kth subcarrier, also by reciprocity, hTT;k, hTR;k as the downlink channels. The received waveform at the receiver side could be expressed as [10]:

$$\mathrm{y_k} = \underbrace{\mathrm{h_{R,k}^T \Psi_k h_{T,k} s_k}}_{\text{LIS-assisted link}} + \underbrace{\mathrm{h_{TR,k} s_k}}_{\text{Direct link}} + \mathrm{n_k} \tag{1}$$

where the matrix Ψ is an M×M , that we call it the LIS interaction matrix with M elements, characterizes the interaction of the LIS with the incident (impinging) signal from the transmitter. h_k , denotes the communication channel with T, and R subindecies denote the transmitter and receiver section respectively. Also, n_k, represents the additive wight Gaussian noise (AWGN) signal for the k^{th} sample. S_k represents the transmitted waveform through the k^{th} subcarrier, and satisfies the per-subcarrier power constraint. Next, the mean square value of S_k might be computed as follows:

$$\mathbb{E}[|\mathrm{s_k}|^2] = \frac{\mathrm{P_T}}{\mathrm{K}} \tag{2}$$

with P_T being the total transmit power, and the receive noise is denoted by n_k.

$$\psi^* = arg \max_{\psi \in \mathcal{P}} \sum_{k=1}^{K} log_2 \,(1 + SNR\left|(h_{T,k} \odot h_{R,k})^T \psi\right|^2 \tag{3}$$

The overall aim of LIS is to interact with all the incident signal (by adjusting k) in a way that optimizes it a specific performance measure such as the system rate that could be achieved or the amount of network coverage. To simplify the design and analysis of the algorithms in this study, we will focus on the case where the direct link does not exist. This represents Scenarios where the direct link is blocked or stopped When the receiving power is negligible compared to that received through the LIS-assisted link. With this assumption, the signal is received it might be expressed as follows [12]:

$$y_k = h_{R,k}^T \Psi_k h_{T,k} s_k + n_k \tag{4}$$

$$y_k = (h_{R,k} \odot h_{T,k})^T \psi_k s_k + n_k \tag{5}$$

The channel model might be expressed as follows:

$$h_{T,d} = \sqrt{\frac{M}{\rho T}} \sum_{l=1}^{L} \alpha_l \, p(dT_S - \tau_l) \; a(\theta_l, \emptyset_l) \tag{6}$$

Where M, denotes the number of channels, ρ, indicates the IRS conductivity$\theta_l, \emptyset_l$, denote the signals and channels phase shifts respectively, , and T, represents the sampling time. The above equation represents the channel characteristics in terms of capacity, attenuation coefficient, phase angles, time delay, sampling time, and power consumed [15]. Thus, the main aim is to plan and construct the LIS (reflection) interaction vector beamforming, in order to maximize the bit rate that might be achieved at the receiving device, which could be formulated as follows:

$$\mathrm{R}^* = \max_{\varphi \in} \frac{1}{\mathrm{K}} \sum_{\mathrm{k}=1}^{\mathrm{K}} \log_2 \left(1 + \mathrm{SNR}\left|(\mathrm{h_{T,k}} \odot \mathrm{h_{R,k}})^{\mathrm{T}} \varphi\right|^2\right) \tag{7}$$

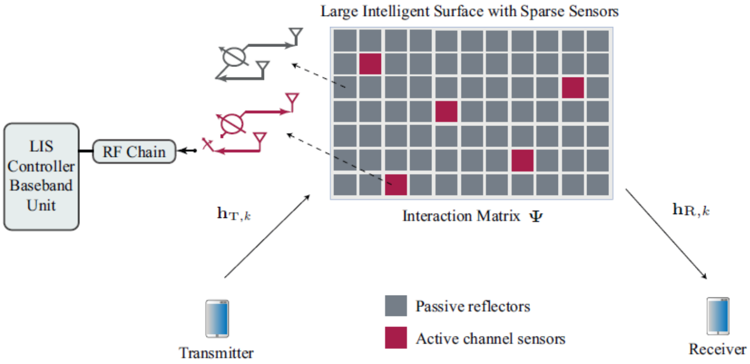

Fig. 2: *A diagram of the adopted system model whereas communication between sender and detector is supported by a large smart surface (no). The LIS reacts to the incident wave through matrix interaction [8].*

The main challenge: as demonstrated in the mathematical equations, is trying to find the optimal reaction vector for large intelligent surfice (LIS) as well to achieve the optimal data transmission rate. This needs a thorough search in the code book. Note that the size of the codebook should usually be in a file having the same order of number of antennas to utilize. This means that the beamforming is a reasonable reflection of the LIS codebook potentially includs thousands of candidate codewords. With such huge codebooks, a solution exhaustive research of the equations is very difficult. More specifically, there are two main ways to perform search in [7].

The objectives of this study are to use deep learning algorithms to allocate resources in a MIMO network with smart reflective surfaces. Also, the study aims to improve the allocation efficiency to the highest percentage while reducing the data flow rate to a minimum to obtain the best performance.

Literature Review

Under different names like reconfigurable intelligent surfaces, intelligent reflecting surfaces, and smart reflect-arrays, LIS-helped remote interchanges have been drawing expanding interest lately. From an execution viewpoint, LIS can be assembled utilizing almost passive components with reconfigurable boundaries [7]. Different LIS plans have been proposed in the literature with more noticeable quality given to software-characterized metamaterials [9], [10] and regular reflect-arrays [6], [8] among others. For that multitude of plans, different signal-processing arrangements have been proposed for optimizing the plan of the LIS interaction matrices. A LIS-helped downlink multiuser arrangement was thought of in [7] with single-antenna clients. Computational low intricacy calculations were then proposed for optimizing the plan of the LIS interaction matrices, utilizing quantized phase shifters/reflectors for demonstrating the LIS components. In [11], an LIS-helpe kilo s.lksxsq' \d downlink scenario was thought of, where both the LIS interaction grid and the base station precoder grid was planned, expecting the situation where a line-of sight (LOS) may exist between the base station and the LIS. In [12], another transmission system consolidating LIS with file, modulation was proposed to work on the framework unearthly effectiveness. As far as the general framework execution, an uplink multiuser scenario was considered in [13] and the information rates were formed for the situation where channel assessment errors exist in the accessible channel information. A downlink LIS-helped multiple-input multiple-output (MIMO) non-orthogonal multiple access (NOMA) system is proposed in [18] for accomplishing higher framework spectrum proficiency gains. The LIS can be utilized for remote localization purposes too; in [19], a LIS-helped downlink millimeter wave (mmWave) positioning issue was examined from the Fisher Data point of view. In light of this examination, a calculation was created for advancing the positioning quality. Deep learning arrangements have been proposed in the literature for tending to configuration challenges in mmWave and massive MIMO frameworks [20]-[22]. In [20], a deep learning based bar expectation arrangement was proposed for conveyed mmWave MIMO frameworks to serve exceptionally versatile clients with irrelevant preparation above and high information rate gains, thought about to coordinate beamforming systems that don't influence AI. In [21], a deep learning based blockage forecast arrangement was proposed to address the unwavering quality and latency difficulties of abrupt blockage of the line-of-sight connect in mmWave MIMO frameworks. A channel covariance expectation arrangement utilizing generative adversarial networks was proposed in [22] for mmWave Massive MIMO frameworks to diminish the preparation above related with getting the channel information. The Basic Test: All the earlier work in [7], [8], [11-13], [18] accepted that the information about the channels between the LIS and the transmitters/beneficiaries is accessible at the base station, either impeccably or with some mistake. Getting this channel information, in any case, is one of the most essential challenges for LIS frameworks due to the massive number of antennas (LIS components) and the hardware imperatives on these components. All the more explicitly, if the LIS components are executed utilizing phase shifters that simply reflect the occurrence signals, then, at that point, there are two primary methodologies for planning the LIS reflection framework. The principal approach is to gauge the LIS-helped channels at the transmitter/collector via preparing every one of the LIS components, regularly individually, and then, at that point, utilize the assessed channels to plan the reflection lattice. This yields a massive channel preparing above due to the exceptionally enormous number of components at the LIS. Rather than the express channel assessment, the LIS reflection the network can be chosen from quantized codebooks by means of online pillar/reflection preparing. This is like the normal pillar preparing strategies in mmWave frameworks that utilize comparative phase shifter models [23], [24]. To quantize adequately the space, in any case, the size of the reflection codebooks needs ordinarily to be in the request for the quantity of antennas, which prompts enormous preparation above. To keep away from this preparing above, a trivial arrangement is to utilize completely computerized or hybrid simple/computerized structures at the LIS, where each antenna component is associated in some way to the baseband where channel assessment techniques can be utilized to get the channels [25-27]. This arrangement, notwithstanding, prompts high hardware intricacy and power utilization due to the massive number of LIS components.

Methodology:

In order to implement the study idea of this article, we propose two types of scenarios, while confirming the assumption that there are only secondary paths represented by the RIS system, and that the direct path is not activated, as is the case in research. To explain the proposed scenarios, we explain them in detail in the following sections.

A) Scenario 1

Assuming that there are k=32 users, then, M= 32*32=1024 reconfigurable elements represeting the various channel paths. Samples number Ns=1000 sample for each k user signal. SNR=10 dB i.e. signal power is 10 times the noise power. Each user signal k, will be multiplied by the IRS matrix, which represents an array of (32 * 32)= 1024 different paths of the channel, so that the values of 1024 matrix are random values representing the levels of transmission channel attenuation due to the multiplicity of paths, so that the length of the resulting signal is for each user will be: The users matrix length =(k*Ns) =32*1000. The RIS channels paths weights matrix= M=(32*32), (32*1000)T.*(32*32)=1000*32 which is the new users sets matrix after passing through the RIS. Thus the new obtained users sets matrix after passing through the RIS will be (1000*32)T=32*1000 vector. Thus the RNN algorithm will have input layer of (32*1000), hidden layer of 32 eurons, and output layer of (32*1000) as shown in Figure 3.

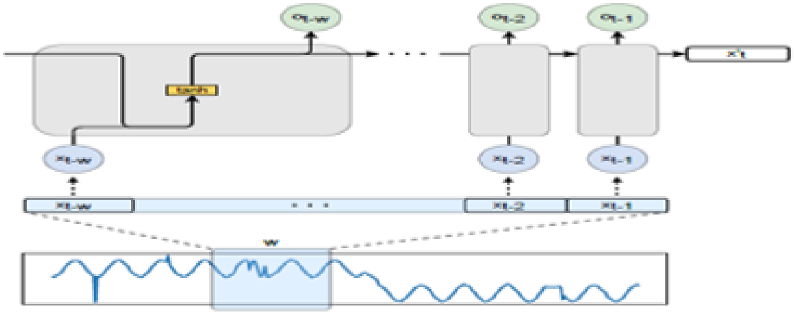

(32*1000) (32 Neurons) (32*1000)

Fig. 3: *The suggested RNN algorithm for scenario 1.*

The resulting output vector must represent the same values as the input vector before it passes through the RIS matrix, meaning that it is inaffected by multipath problems and that the value of the bit error rate is very small, as explained in the previous equations.

B) Scenario 2

Assuming that there are k=32 users, then, M= 32*32=1024 reconfigurable elements represeting the various channel paths. Samples number Ns=1000 sample for each k user signal. SNR=10 dB i.e. signal power is 10 times the noise power. Each user signal k, will be multiplied by the IRS matrix, which represents an array of (32 * 32)= 1024 various paths of the channel, so that the values of 1024 matrix are random values representing the levels of transmission channel attenuation due to the multiplicity of paths, so that the length of the resulting signal is for each user will be: Each users vector length =(1*Ns) =1*1000. The RIS channels paths weights matrix= M=(32*32)=1024, and each element will be multiplied by each user vector, thus 1024*1*1000=1024*1000 case for each transmitted user. Thus the suggested neural algorithm will have input layer of (1024*1000), hidden layer of 1024 neurons, and the output layer of (1024*1000) as shown in Figure 4.

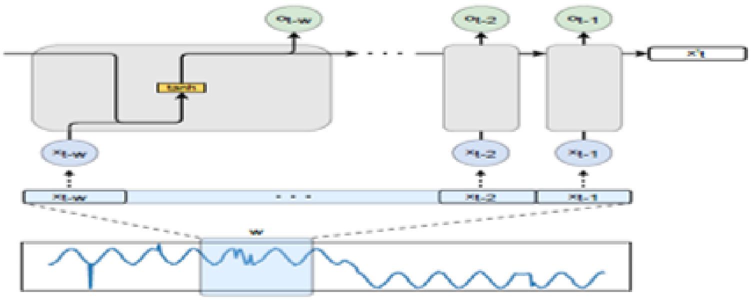

(1024*1000) (1024 Neurons) (1024*1000)

Fig. 4: *The suggested RNN algorithm for scenario 1.*

The resulting output vector must represent the same values as the input vector before it passes through the RIS matrix, meaning that it is inaffected by multipath problems and that the value of the bit error rate is very small, as explained in the previous equations.

C) Structure of Emploed DataSet

In this research, the necessary data necessary to train the proposed deep learning algorithms RNN and LSTM are generated through a program dedicated to implementing the requirements of this data. The program creates the required data in the form of embedded communications signals for each user out of k = 32 users, so that the length of each user wave is Ns = 1000 samples. The data required for this study will be generated as a matrix with a capacity of (32*1000), where the rows of the matrix represent the waves of users and its columns represent the number of users. Figure 5 shows a snapshot of the data generated for the user group to train the deep learning algorithms.

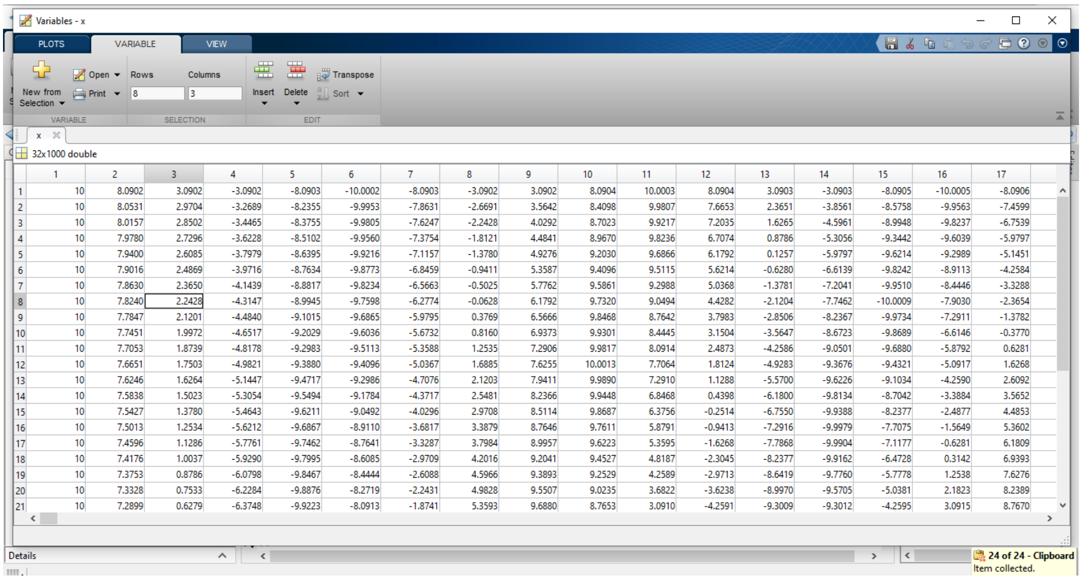

32x1000 double

	1	2	3	4	5	6	7	8	9	10	11	12	13	14	15	16	17
1	10	8.0902	3.0902	-3.0902	-8.0903	-10.0002	-8.0903	-3.0902	3.0902	8.0904	10.0003	8.0904	3.0903	-3.0903	-8.0905	-10.0005	-8.0906
2	10	8.0531	2.9704	-3.2689	-8.2355	-9.9953	-7.8631	-2.6691	3.5642	8.4098	9.9807	7.6653	2.3651	-3.8561	-8.5758	-9.9563	-7.4599
3	10	8.0157	2.8502	-3.4465	-8.3755	-9.9805	-7.6247	-2.2428	4.0292	8.7023	9.9217	7.2035	1.6265	-4.5961	-8.9948	-9.8237	-6.7539
4	10	7.9780	2.7296	-3.6228	-8.5102	-9.9560	-7.3754	-1.8121	4.4841	8.9670	9.8236	6.7074	0.8786	-5.3056	-9.3442	-9.6039	-5.9797
5	10	7.9400	2.6085	-3.7979	-8.6395	-9.9216	-7.1157	-1.3780	4.9276	9.2030	9.6866	6.1792	0.1257	-5.9797	-9.6214	-9.2989	-5.1451
6	10	7.9016	2.4869	-3.9716	-8.7634	-9.8773	-6.8459	-0.9411	5.3587	9.4096	9.5115	5.6214	-0.6280	-6.6139	-9.8242	-8.9113	-4.2584
7	10	7.8630	2.3650	-4.1439	-8.8817	-9.8234	-6.5663	-0.5025	5.7762	9.5861	9.2988	5.0368	-1.3781	-7.2041	-9.9510	-8.4446	-3.3288
8	10	7.8240	2.2428	-4.3147	-8.9945	-9.7598	-6.2774	-0.0628	6.1792	9.7320	9.0494	4.4282	-2.1204	-7.7462	-10.0009	-7.9030	-2.3654
9	10	7.7847	2.1201	-4.4840	-9.1015	-9.6865	-5.9795	0.3769	6.5666	9.8468	8.7642	3.7983	-2.8506	-8.2367	-9.9734	-7.2911	-1.3782
10	10	7.7451	1.9972	-4.6517	-9.2029	-9.6036	-5.6732	0.8160	6.9373	9.9301	8.4445	3.1504	-3.5647	-8.6723	-9.8689	-6.6146	-0.3770
11	10	7.7053	1.8739	-4.8178	-9.2983	-9.5113	-5.3588	1.2535	7.2906	9.9817	8.0914	2.4873	-4.2586	-9.0501	-9.6880	-5.8792	0.6281
12	10	7.6651	1.7503	-4.9821	-9.3880	-9.4096	-5.0367	1.6885	7.6255	10.0013	7.7064	1.8124	-4.9283	-9.3676	-9.4321	-5.0917	1.6268
13	10	7.6246	1.6264	-5.1447	-9.4717	-9.2986	-4.7076	2.1203	7.9411	9.9890	7.2910	1.1288	-5.5700	-9.6226	-9.1034	-4.2590	2.6092
14	10	7.5838	1.5023	-5.3054	-9.5494	-9.1784	-4.3717	2.5481	8.2366	9.9448	6.8468	0.4398	-6.1800	-9.8134	-8.7042	-3.3884	3.5652
15	10	7.5427	1.3780	-5.4643	-9.6211	-9.0492	-4.0296	2.9708	8.5114	9.8687	6.3756	-0.2514	-6.7550	-9.9388	-8.2377	-2.4877	4.4853
16	10	7.5013	1.2534	-5.6212	-9.6867	-8.9110	-3.6817	3.3879	8.7646	9.7611	5.8791	-0.9413	-7.2916	-9.9979	-7.7075	-1.5649	5.3602
17	10	7.4596	1.1286	-5.7761	-9.7462	-8.7641	-3.3287	3.7984	8.9957	9.6223	5.3595	-1.6268	-7.7868	-9.9904	-7.1177	-0.6281	6.1809
18	10	7.4176	1.0037	-5.9290	-9.7995	-8.6085	-2.9709	4.2016	9.2041	9.4527	4.8187	-2.3045	-8.2377	-9.9162	-6.4728	0.3142	6.9393
19	10	7.3753	0.8786	-6.0798	-9.8467	-8.4444	-2.6088	4.5966	9.3893	9.2529	4.2589	-2.9713	-8.6419	-9.7760	-5.7778	1.2538	7.6276
20	10	7.3328	0.7533	-6.2284	-9.8876	-8.2719	-2.2431	4.9828	9.5507	9.0235	3.6822	-3.6238	-8.9970	-9.5705	-5.0381	2.1823	8.2389
21	10	7.2899	0.6279	-6.3748	-9.9223	-8.0913	-1.8741	5.3593	9.6880	8.7653	3.0910	-4.2591	-9.3009	-9.3012	-4.2595	3.0915	8.7670

Fig. 5: *Snapshot of the dataset generated for the user group to train the deep learning algorithms.*

The structure of the suggested IRS model using deep learning technique is also demonstrated in Figure 6.

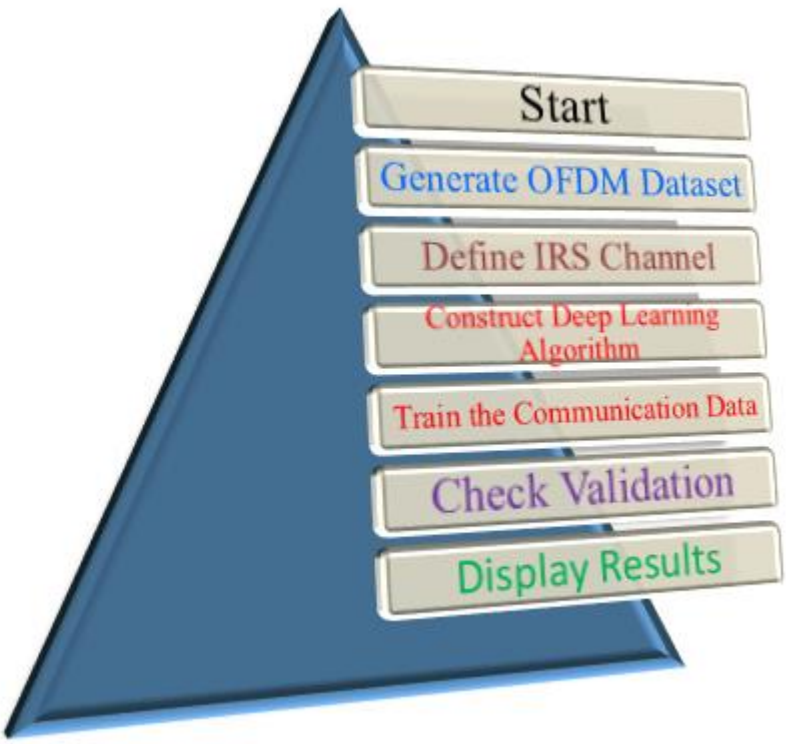

Fig. 6: *Demonstration of the structure of the suggested IRS model using deep learning technique.*

By looking at Figure 6 above, the signal flow diagram for the model proposed in the study begins with identifying and creating a data set of communications signals including OFDM, which will be used to transmit information through the IRS communications channel. This is followed by defining the IRS channel according to the equations explained in the first part of this research. After that, the structure of building a deep learning algorithm of the LSTM type is called to simulate the inverse and equalization of the effect of communication channels. Also, the smart algorithm model is trained using the telecommunications data used in this study, and then they conduct verification of the authenticity of the receipt of the original data, and finally the results are displayed. Moreover, the detailed proposed deep learning RNN-LSTM algorithm structure is displayed in Figure 7.

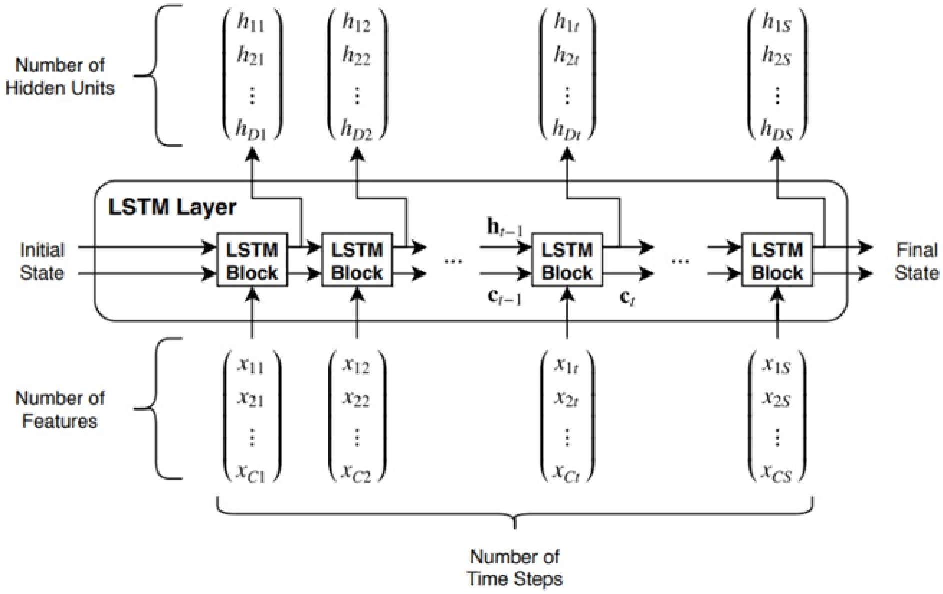

Fig. 7: *The proposed DL (RNN) (LSTM) algorithm structure.*

This diagram shows the progression of a period series X with C features (channels) of length S through a LSTM layer. In the outline, ht And ct mean the result (otherwise called hidden state) and cell state at time step t, separately. The main LSTM block utilizes the network's underlying state and the sequence's first-time move toward compute the principal yield and the refreshed cell state. At time step t, the block utilizes the present status of the network (ct−1 ht−1) and the following stage in the sequence is to work out the result and the refreshed cell state ct. The layer state comprises of the hidden state (the result state) and the cell state. The hidden state at time step t contains the results of the LSTM layer for that time step. The cell state contains data gained from past time steps. At each time step, the layer adds or eliminates data from the cell state. The layer controls these updates utilizing passages. The accompanying parts control the cell state and hidden state of the layer.

Results & Discussion:

This section presents the results of a study conducted on deep learning algorithms related to resource allocation in MIMO networks involving smart reflective surfaces. A MATLAB software application was employed to create a simulation environment featuring a multi-input multiple-output (MIMO) network including smart reflective surfaces (IRS). This study used simulation-based experiments as a research methodology with LSTM-RNN deep learning algorithms for training and testing procedures using a dataset produced in a MATLAB simulation environment. The effectiveness of the suggested technique was evaluated through various metrics, including spectral efficiency, power efficiency, and bit error rate. This section also provides an overview of the data used in the study. Deep learning algorithms are trained and tested using data generated from the simulation environment, which consists of a dataset related to system parameters and configurations, along with proposed performance metrics. The data set is divided into two main subsets, the training set and the test set, in a ratio of 70:30. The largest subset, representing 70% of the data, is used for training purposes, and the remaining 30% is reserved for testing model performance. The MATLAB simulation environment, along with 5G Toolbox and Deep Learning Toolbox, was used to perform the simulations. The study evaluated the effectiveness of the suggested technology and a simulation analysis study was carried out to configure a multi-input multiple-output (MIMO) network. In fact, eight client devices with a base station and an intelligent intermediate reflective surface (IRS) have been considered. The achieved results were analyzed in an organized and systematic manner. The operational setup of the system is frequency-selective fading, and both the base station and the receiving station have knowledge of the channel state information (CSI). Evaluation of the deep learning-based method with respect to the overall rate capability of the network is performed. The results indicate that the proposed methodology shows superior performance compared to the RB and WSR algorithms, as it achieves greater overall capacity under identical channel conditions. The simulation model of the smart IRS interaction matrix was implemented with the loaded dataset using the proposed RNN-LSTM network technique. The layers of the simulated RNN-LSTM network are shown in Figure 8.

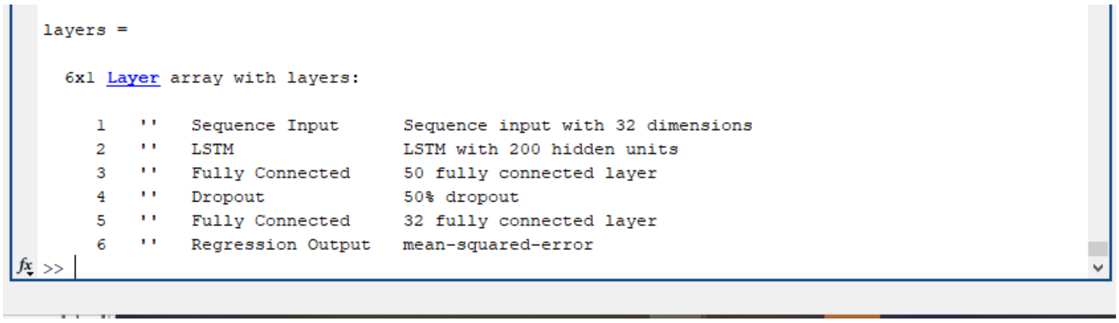

Fig. 8: *The simulated RNN-LSTM network layers.*

Regarding Figure 8, we might recognize the details of the proposed RNN-LSTM network strategy that contain a sequence input layer with 32 dimensions, followed by the LSTM layer 200 hidden units. the third layer is the dropout layer with 50% dropout, and next fully connected layer with 50 fully connected layer ended by the regression layer with mean square error. Also, the trainning options of the suggested deep learning network are presented in Figure 8.

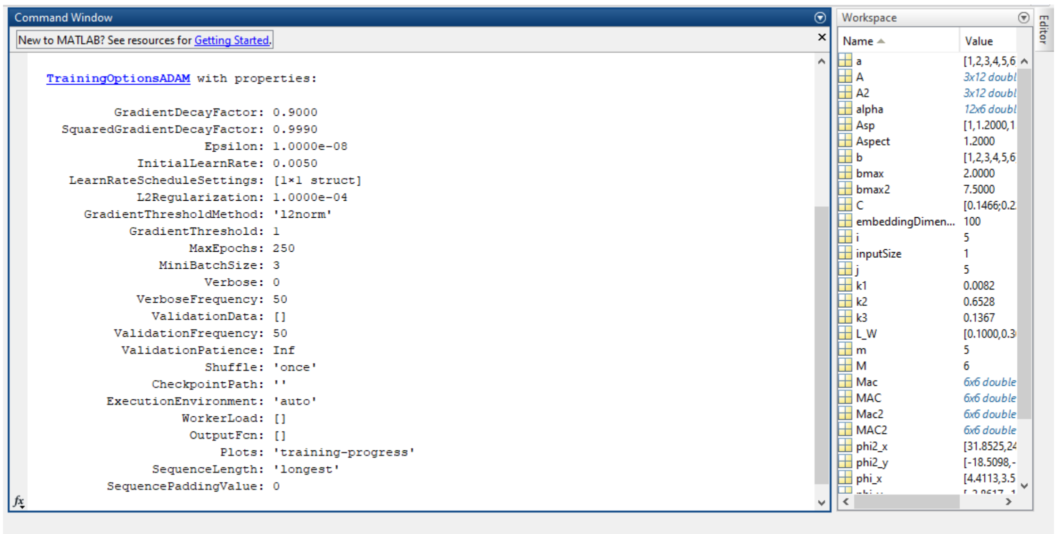

Fig 9: *Trainning network simulated RNN-LSTM network layers.*

By looking at the details of Figure 9, we notice that the training options explain all the details of training the proposed smart algorithm network. By adjusting the training options settings, the training mechanism will be adjusted to control the number of training repetitions, the time distances between training models, the methods for displaying training results, the minimum and maximum display of training distances, the speed of the training rate, and other details that control the nature of the training options on Smart grid. Which affects the results of training. Then, recalling the details of the training scenarios for the proposed IRS interaction channel model discussed earlier, we analyze the sequences of the input sent dataset of the trained model represented by K = 32 users or agents, each one digitally sending problem signals with N = 1000 Sample channel-passed Additive White Gaussian Noise (AWGN) and IRS matrix models. The sequences of the sent customer data set passed from the IRS matrix are shown in Figure 10 without and with the influence of AWGN.

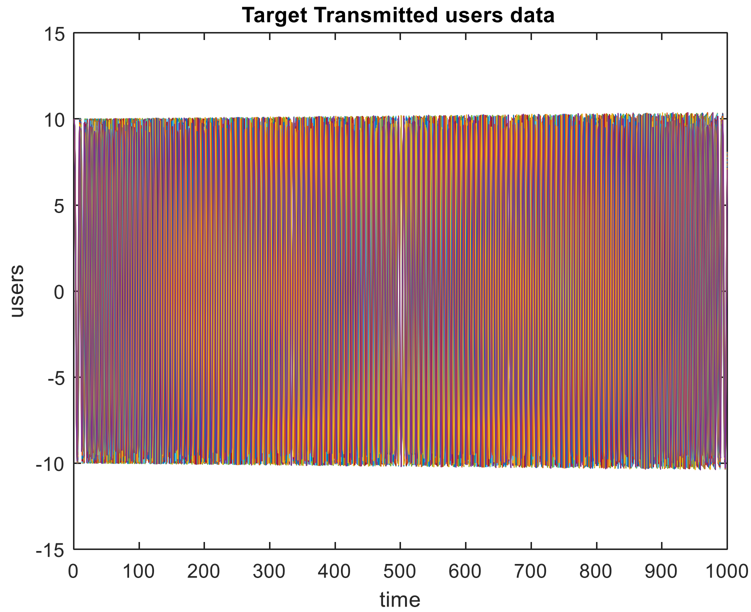

(a)

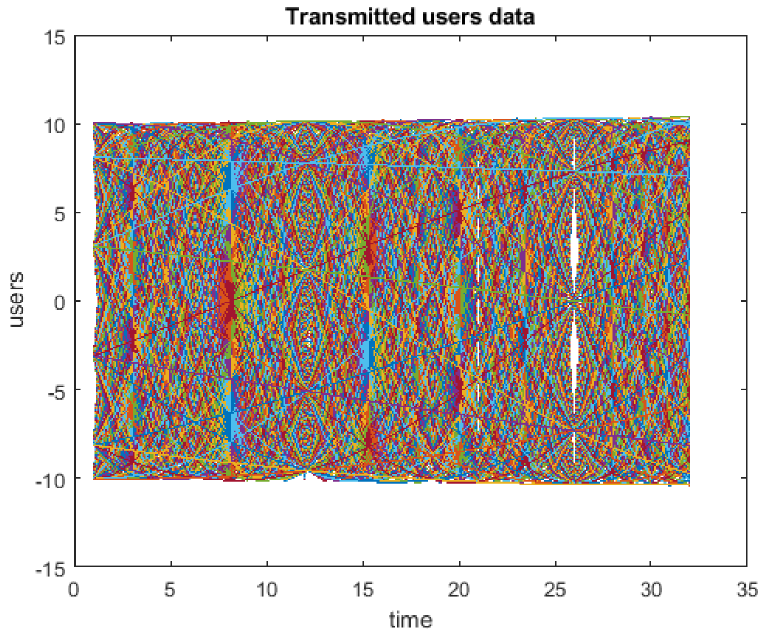

(b)

Fig. 10: *The transmitted clients dataset sequences passed from the IRS matrix, (a) Without AWGN, (b) With AWGN.*

We notice by looking at Figure 10 that the set of information patterns of users' transmission waves appears as overlapping waves containing 1000 patterns per user, with 32 clients, the amplitude ranges from -10 to 10, as shown in the figure above. One could further observe the effect of the Gaussian transmission channel on the transmitted data set, so that the data is lined up and regular, as shown in Figure 10.(a), while the effect of noise and interference of the transmitted data increases, as shown in Figure 10.(b). Moreover, regarding the target sender user datasets which should be discovered at the receiving end of the proposed IRS model, which also consist of K-32 users with N = 1000 samples as shown in Figure 11 also without and with the effect of AWGN.

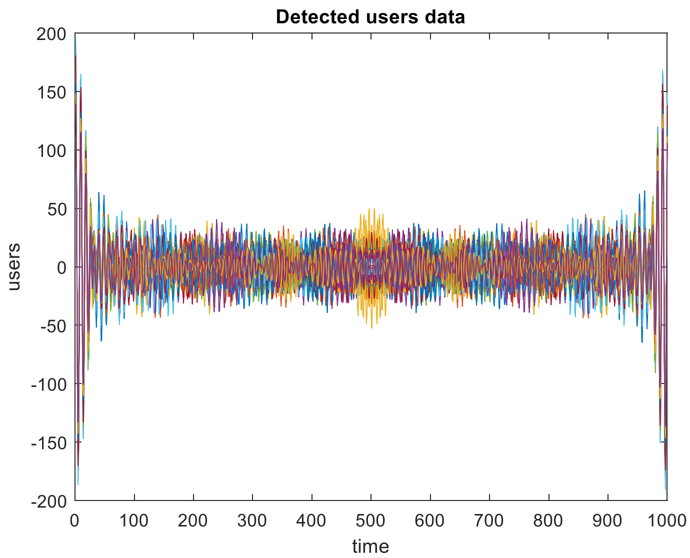

(a)

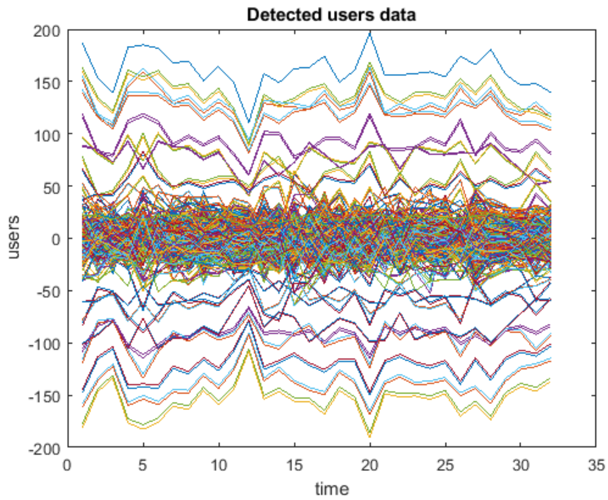

(b)

Fig. 10: *The detected clients dataset sequences after passing from the IRS matrix channels, (a) Without AWGN, (b) With AWGN.*

Furthermore, by recognizing Figure 11, one could notice that the set of received customer data set wave sequences passed from the IRS matrix channels appear as distorted waves containing 1000 samples per user, with 32 users, ranging from -10 to 10 in power, as Shown in the figure above. In fact, this distortion and decay resulting in the received user data set after passing through the interlaced channels represents the effect of these channels on the transmission values of each user wave as a result of the effect of multiple transmission channels and the bounce of transmission waves with several effects represented by the interlaced matrix (IRS). Now, after using the proposed RNN-LSTM network training process in the applied scenario, the IRS Smart Interactive Channels model training results are shown in Figure 12.

```
Command Window
New to MATLAB? See resources for Getting Started.

layers =

  6x1 Layer array with layers:

     1   ''   Sequence Input      Sequence input with 32 dimensions
     2   ''   LSTM                LSTM with 200 hidden units
     3   ''   Fully Connected     50 fully connected layer
     4   ''   Dropout             50% dropout
     5   ''   Fully Connected     32 fully connected layer
     6   ''   Regression Output   mean-squared-error
Training on single CPU.
|========================================================================================|
|  Epoch  |  Iteration  |  Time Elapsed  |  Mini-batch  |  Mini-batch  |  Base Learning  |
|         |             |   (hh:mm:ss)   |     RMSE     |     Loss     |      Rate       |
|========================================================================================|
|       1 |           1 |       00:00:02 |        40.45 |        818.1 |          0.0050 |
|      50 |          50 |       00:01:01 |        32.01 |        512.4 |          0.0050 |
|     100 |         100 |       00:01:59 |        28.18 |        397.0 |          0.0050 |
|     150 |         150 |       00:03:01 |        26.68 |        355.9 |          0.0050 |
|     200 |         200 |       00:04:05 |        25.44 |        323.6 |          0.0050 |
|     250 |         250 |       00:05:24 |        25.56 |        326.8 |          0.0050 |
|========================================================================================|
```

Fig.12: *The results of the smart IRS interacted channels model trainning.*

By observing Figure 12, the resulting table shows the training results of the proposed intelligence network, where details show the number of iterations 250 iterations, the amount of elapsed time = 5 minutes, the minimum batch (root mean square error) = 25.56, and the minimum loss Batch=326.8, base learning rate=0.005. Now, the results of the trainning progress curves are displayed for bothe the trainning accuracy and overall loss in Figure 13.

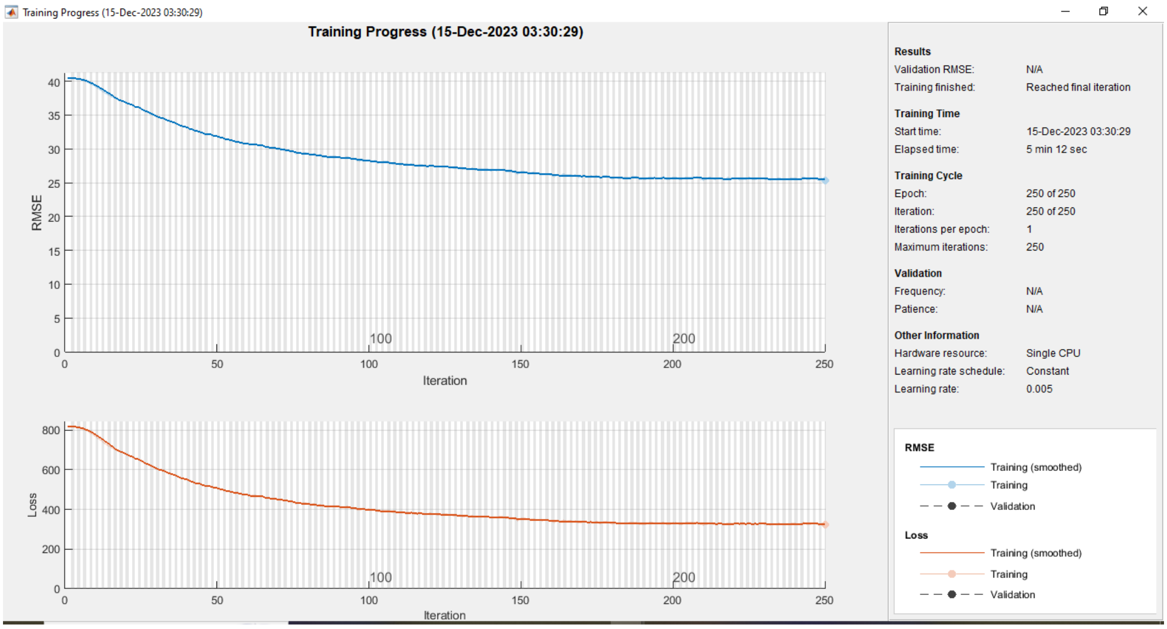

Fig. 13: *The results of the trainning progress curves are displayed for bothe the trainning accuracy and overall loss.*

From reviewing Figure 13, we greatly estimate how much the algorithmic network intelligence trains over the duration and training periods, where results occur with a minimum batch loss (rms error) starting with 40 and ending with 25.56, versus a minimum batch loss starting with 800 and ends with 326.8. After completing the training operations of the proposed intelligent algorithm network, the training results of the resulting detected dataset will appear after passing through the proposed RNN-LSTM algorithm network, which is displayed as shown in Figure 13 without AWGN and with AWGN effects. Finally, we can find the cumulative error plots and the final accuracy for the network operation level of the suggested deep learning algorithm by calculating the difference among the received results and the originally sent target results, as shown in Figure 14.

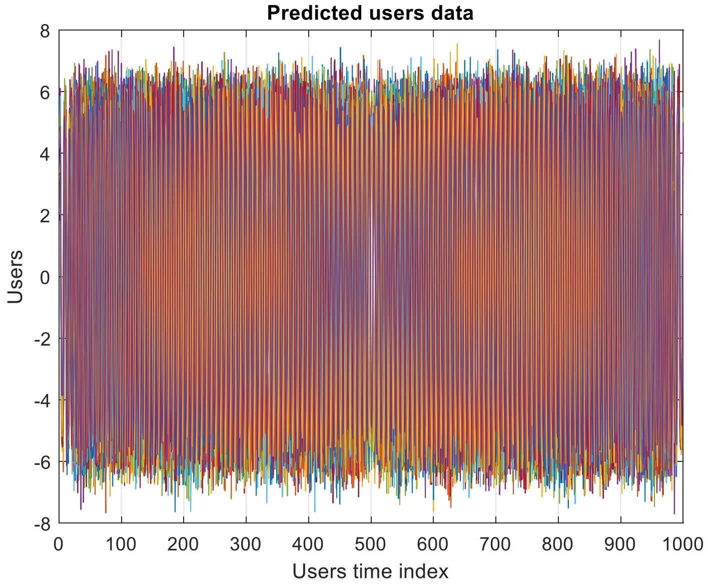

(a)

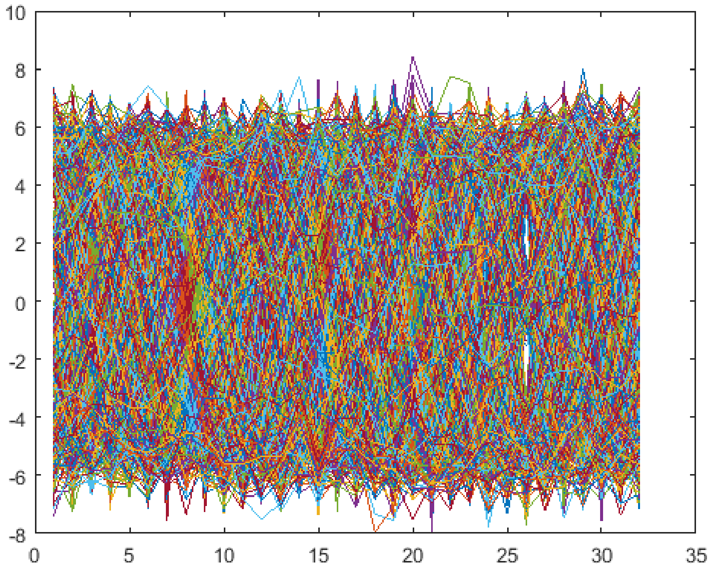

(b)

Fig. 14: *The results of training the detected data set as appeared after passing through the proposed RNN-LSTM algorithm network without AWGN and with AWGN effects, (a) Without AWGN, (b) With AWGN effect.*

By reviewing the results of training the data set using the proposed intelligence algorithm, we notice that the received data sets have been excluded from the effects of interlaced channels represented by the IRS matrix, so that the results appear pure and free of decay and distortions, especially if the effect of noise is not taken into account in Figure 14. The results also appear with deformities simple and acceptable, considering the noise effects in Figure 14. This indicates the success of the proposed deep learning algorithm network technique in training the data and eliminating the effects of the correlation channels represented by the IRS matrix. Moreover, the predicted and training error signals have been achieved as presented in Figure 15.

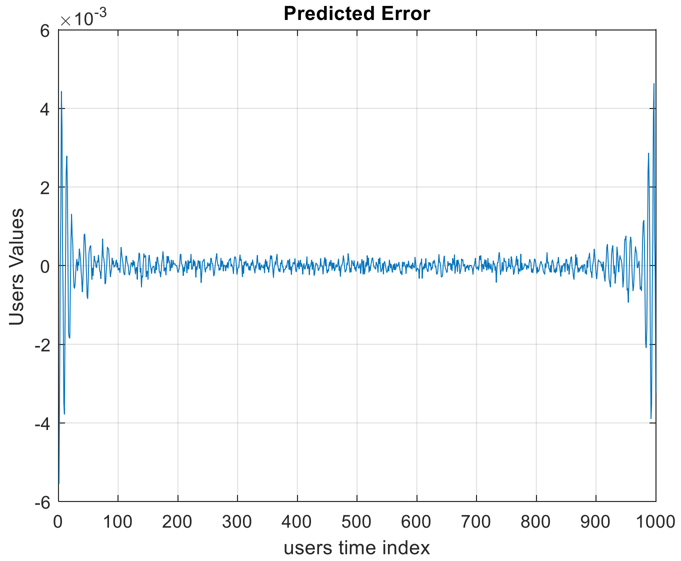

(a)

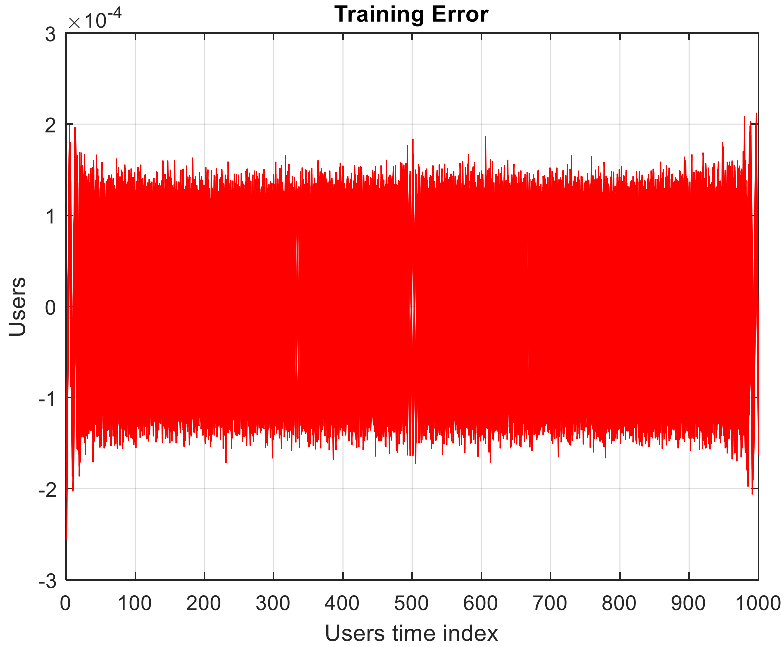

(b)

Fig.15: *The results of training the detected data set as appeared after passing through the proposed RNN-LSTM algorithm network without AWGN and with AWGN effects, (a) Without AWGN, (b) With AWGN effect.*

Furthermore, the predicted and traininmg accuracy of the suggested deep earning IRS model have computed as displayed in Figure 16.

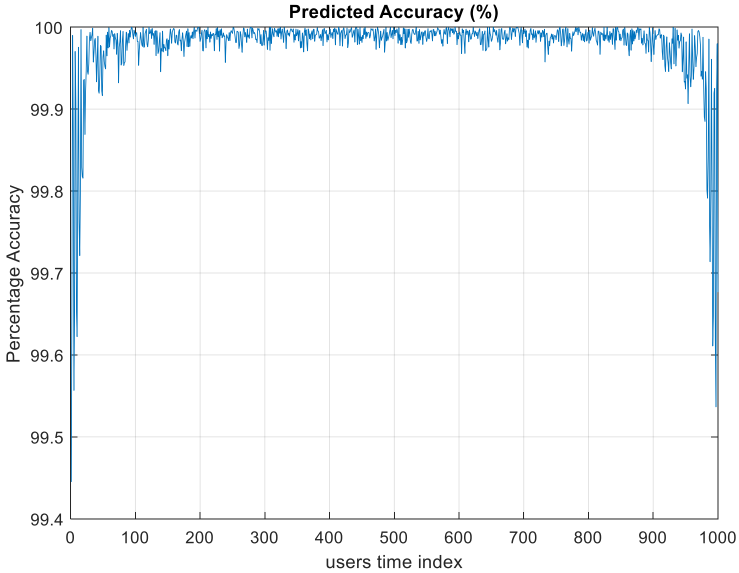

(a)

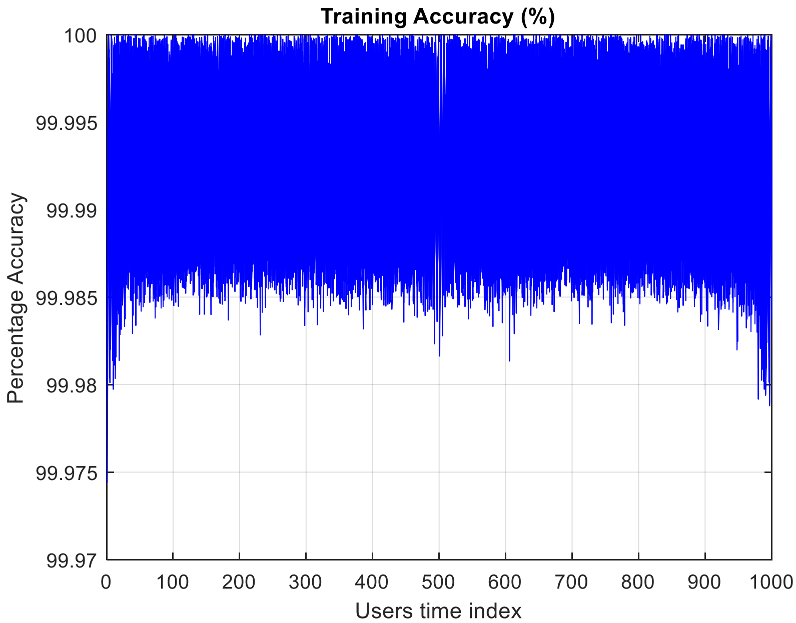

(b)

Fig 16: *The results of training the detected data set as appeared after passing through the proposed RNN-LSTM algorithm network without AWGN and with AWGN effects, (a) Without AWGN, (b) With AWGN effect.*

Also, by observing the training results of the data set trained using the proposed intelligence algorithm, we notice that the accumulated error results charts give very low percentages, reaching a maximum of 0.0002. Also, the final accuracy results reach high percentages exceeding 99.97%, and this indicates the success of the technique. The proposed deep learning algorithm network trains data and eliminates the effects of engagement channels represented by the IRS matrix. Finally, for results validation, Table 1 shows the comparison among the achieved results with and without deep learning technique.

Table 1: Comparison of the achieved results

System Type	SNR (dB)	BER	Error Rate	Efficiency	Precesion
Without DL	10	10-1	25-26%	80%	85%
	50	10-2	20-21%	90%	91%
With DL	1	10-4	11%	99.8%	98.875%

Conclusions

In this paper, deep learning algorithms have been investigated for improving resource allocation in multiple-input multiple-output (MIMO) networks engaged with intelligent reflective surfaces (IRS). The suggested deep learning RNN-LSTM algorithm trains the data and removes the effects of other sharing channels. In summary, our research focused on the capabilities of the deep learning algorithms in monetizing smart reflective surfaces in the context of resource allocation within MIMO networks. The suggested methodology has the potential for further improvements and customizations to accommodate diverse network structures and variables, thus opening prospects for further investigation in this area. The results of the simulation study indicate that the proposed methodology shows superior performance. These results have compared to existing technique as presented by the network performance metrics of spectral efficiency and energy efficiency. Moreover, the implementation of smart reflective surfaces has been shown to have a noticeable impact on resource allocation, especially in cases where resources are limited. Through the training results of the dataset, we notice that the accumulated error results plots provide very low percentages, reaching a maximum of 0.0002. The final accuracy results also reach high rates exceeding 99.97%, and this indicates the success of such technology.

References

1. W. A. Gardner, “Exploitation of spectral redundancy in cyclostationary signals,” IEEE Signal Process. Mag., [31] S. Foo, “Liquid-crystal Reconfigurable Metasurface Reflectors,” in Proc. of IEEE International Symposium on Antennas and Propagation USNC/URSI, July 2017, pp. 2069–2070.
2. Q. Wu and R. Zhang, “Intelligent Reflecting Surface Enhanced Wireless Network via Joint Active and Passive Beamforming,” IEEE Transactions on Wireless Communications, vol. 18, no. 11, pp. 5394–5409, 2019.
3. A. Alkhateeb, “DeepMIMO: A Generic Deep Learning Dataset for Millimeter Wave and Massive MIMO Applications,” in Proc. of Information Theory and Applications Workshop (ITA), San Diego, CA, Feb 2019, pp. 1–8. [Online]. Available: https://www.deepmimo.net/
4. C. Rusu, N. Gonzalez-Prelcic, and R. W. Heath, “Algorithms for the Construction of Incoherent Frames under Various Design Constraints,” Signal Processing, vol. 152, pp. 363 – 372, 2018.
5. A. Taha, Y. Zhang, F. B. Mismar, and A. Alkhateeb, “Deep Reinforcement Learning for Intelligent Reflecting Surfaces: Towards Standalone Operation,” in Proc. of IEEE International Workshop on Signal Processing Advances in Wireless Communications (SPAWC), May 2020, pp. 1–5.
6. S. V. Hum and J. Perruisseau-Carrier, “Reconfigurable Reflectarrays and Array Lenses for Dynamic Antenna Beam Control: A Review,” IEEE Transactions on Antennas and Propagation, vol. 62, no. 1, pp. 183–198, Jan 2014.

7. C. Huang, A. Zappone, G. C. Alexandropoulos, M. Debbah, and C. Yuen, “Reconfigurable Intelligent Surfaces for Energy Efficiency in Wireless Communication,” IEEE Transactions on Wireless Communications, 2019.
8. X. Tan, Z. Sun, D. Koutsonikolas, and J. M. Jornet, “Enabling Indoor Mobile Millimeter-wave Networks Based on Smart Reflect-arrays,” in Proc. of IEEE International Conference on Computer Communications (INFOCOM), April 2018, pp. 270–278.
9. Y. Zhang, J. Zhang, Y.Wang, Z. Yu, and B. Zhang, “A 4-bit Programmable Metamaterial Based on VO2Mediums,” in Proc. of IEEE/MTT-S International Microwave Symposium (IMS), June 2018, pp. 984–986.
10. C. Liaskos, S. Nie, A. Tsioliaridou, A. Pitsillides, S. Ioannidis, and I. Akyildiz, “A New Wireless Communication Paradigm through Software-Controlled Metasurfaces,” IEEE Communications Magazine, vol. 56, no. 9, pp. 162–169, Sep. 2018.
11. Q.-U.-A. Nadeem, A. Kammoun, A. Chaaban, M. Debbah, and M.-S. Alouini, “Large Intelligent Surface Assisted MIMO Communications,” arXiv preprint arXiv:1903.08127, Mar 2019.
12. E. Basar, “Large Intelligent Surface-Based Index Modulation: A New Beyond MIMO Paradigm for 6G,” arXiv e-prints, p. arXiv:1904.06704, Apr 2019.
13. M. Jung, W. Saad, Y. Jang, G. Kong, and S. Choi, “Performance Analysis of Large Intelligent Surfaces (LISs): Asymptotic Data Rate and Channel Hardening Effects,” arXiv preprint arXiv:1810.05667, Oct 2018.
14. A. Faisal, H. Sarieddeen, H. Dahrouj, T. Y. Al-Naffouri, and M.-S. Alouini, “Ultra-Massive MIMO Systems at Terahertz Bands: Prospects and Challenges,” arXiv e-prints, p. arXiv:1902.11090, Feb 2019.
15. E. De Carvalho, A. Ali, A. Amiri, M. Angjelichinoski, and J. Heath, Robert W., “Non-Stationarities in Extra-Large Scale Massive MIMO,” arXiv e-prints, p. arXiv:1903.03085, Mar 2019.
16. E. Björnson, L. Sanguinetti, H.Wymeersch, J. Hoydis, and T. L. Marzetta, “Massive MIMO is a Reality - What is Next? Five Promising Research Directions for Antenna Arrays,” arXiv e-prints, p. arXiv:1902.07678, Feb 2019.
17. L. Sanguinetti, E. Björnson, and J. Hoydis, “Towards Massive MIMO 2.0: Understanding Spatial Correlation, Interference Suppression, and Pilot Contamination,” arXiv e-prints, p. arXiv:1904.03406, Apr 2019.
18. X. Mu, Y. Liu, L. Guo, J. Lin, and N. Al-Dhahir, “Exploiting Intelligent Reflecting Surfaces in NOMA Networks: Joint Beamforming Optimization,” IEEE Transactions on Wireless Communications, vol. 19, no. 10, pp. 6884–6898, 2020.
19. H. Wymeersch and B. Denis, “Beyond 5G Wireless Localization with Reconfigurable Intelligent Surfaces,” in Proc. of IEEE International Conference on Communications (ICC), Jun. 2020, pp. 1–6.
20. A. Alkhateeb, S. Alex, P. Varkey, Y. Li, Q. Qu, and D. Tujkovic, “Deep Learning Coordinated Beamforming for Highly-Mobile Millimeter Wave Systems,” IEEE Access, vol. 6, pp. 37 328–37 348, 2018.
21. A. Alkhateeb, I. Beltagy, and S. Alex, “Machine Learning for Reliable Mmwave Systems: Blockage Prediction and Proactive Handoff,” in Proc. of IEEE Global Conference on Signal and Information Processing (GlobalSIP), Nov 2018, pp. 1055–1059.

22. X. Li, A. Alkhateeb, and C. Tepedelenlioglu, "Generative Adversarial Estimation of Channel Covariance in Vehicular Millimeter Wave Systems," in Proc. of Asilomar Conference on Signals, Systems, and Computers, Oct 2018, pp. 1572–1576.
23. J. Wang, Z. Lan, C. Pyo, T. Baykas, C. Sum, M. Rahman, J. Gao, R. Funada, F. Kojima, H. Harada et al., "Beam Codebook Based Beamforming Protocol for Multi-Gbps Millimeter-Wave WPAN Systems," IEEE Journal on Selected Areas in Communications, vol. 27, no. 8, pp. 1390–1399, Nov. 2009.
24. S. Hur, T. Kim, D. Love, J. Krogmeier, T. Thomas, and A. Ghosh, "Millimeter Wave Beamforming for Wireless Backhaul and Access in Small Cell Networks," IEEE Transactions on Communications, vol. 61, no. 10, pp. 4391–4403, Oct. 2013.
25. A. Alkhateeb, J. Mo, N. Gonzalez-Prelcic, and R. W. Heath, "MIMO Precoding and Combining Solutions for Millimeter-Wave Systems," IEEE Communications Magazine,, vol. 52, no. 12, pp. 122–131, Dec. 2014.
26. R. W. Heath, N. Gonzalez-Prelcic, S. Rangan, W. Roh, and A. M. Sayeed, "An Overview of Signal Processing Techniques for Millimeter Wave MIMO Systems," IEEE Journal of Selected Topics in Signal Processing, vol. 10, no. 3, pp. 436–453, April 2016.
27. A. Alkhateeb, O. El Ayach, G. Leus, and R. W. Heath, "Channel Estimation and Hybrid Precoding for Millimeter Wave Cellular Systems," IEEE Journal of Selected Topics in Signal Processing, vol. 8, no. 5, pp. 831–846, Oct. 2014.